Impacts of shearing and temperature on sewage sludge
Rheological characterisation and integration to flow assessment

Wei, Peng; Uijttewaal, Wim; van Lier, Jules B.; de Kreuk, Merle

DOI
10.1016/j.scitotenv.2021.145005

Publication date
2021

Document Version
Final published version

Published in
Science of the Total Environment

Citation (APA)
Wei, P., Uijttewaal, W., van Lier, J. B., & de Kreuk, M. (2021). Impacts of shearing and temperature on sewage sludge: Rheological characterisation and integration to flow assessment. *Science of the Total Environment*, *774*, 1-9. Article 145005. https://doi.org/10.1016/j.scitotenv.2021.145005

Science of the Total Environment 774 (2021) 145005

Contents lists available at ScienceDirect

Science of the Total Environment

journal homepage: www.elsevier.com/locate/scitotenv

Impacts of shearing and temperature on sewage sludge: Rheological characterisation and integration to flow assessment

Peng Wei [a,b,*], Wim Uijttewaal [c], Jules B. van Lier [a], Merle de Kreuk [a]

[a] Delft University of Technology, Department of Water Management, Stevinweg 1, 2628 CN Delft, the Netherlands
[b] Delft University of Technology, Department of Chemical Engineering, van der Maasweg 9, 2629, HZ, Delft, the Netherlands
[c] Delft University of Technology, Department of Hydraulic Engineering, Stevinweg 1, 2628 CN Delft, the Netherlands

HIGHLIGHTS

- Two rheological states were quantified to characterise sewage sludge thixotropy.
- Temperature impact on rheology was striking, strongly correlated to solids content.
- Difference in master curves implied force equilibrium difference in sludge matrix.
- Rheological discrepancy between the two states was reflected in pipe flow behaviour.
- Pressure drop was well assessed using an 'effective' rheological model for WAS.

GRAPHICAL ABSTRACT

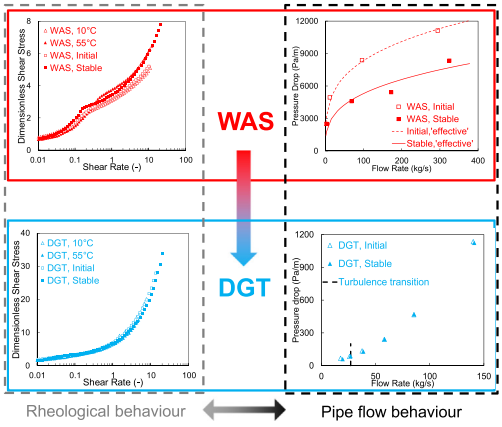

ARTICLE INFO

Article history:
Received 16 September 2020
Received in revised form 2 January 2021
Accepted 2 January 2021
Available online 2 February 2021

Editor: Yifeng Zhang

Keywords:
Sewage sludge
Rheology
Thixotropy
Temperature
Computational fluid dynamics (CFD)
Pipe flow

ABSTRACT

Accurate rheological characterisation of sewage waste activated sludge (WAS) is of high importance for downstream processing related to optimised sludge pumping and mixing, assessment of energy demands and overall process design. However, to elaborate rheological behaviour is often challenging under dynamic operational conditions in practice. In this study, two practical influencing factors were investigated: long-term shearing and temperature. Compared to anaerobic digestate (DGT), concentrated WAS had more complex and stronger thixotropic behaviour. Under the long-term shearing conditions, the sludge thixotropic behaviour was well characterised by two quantified limitation states. Temperature had a striking impact on the rheological properties, which was strongly correlated to solids content and digestion process. The impact discrepancy between the long-term shearing and temperature, implied different mechanisms to shift the equilibrium of hydrodynamic and non-hydrodynamic interactions for structure deformation and recovery. The distinct rheological properties between the two determined states were clearly reflected in pipe flow behaviour, revealing a concrete link between lab-measured sludge rheology and its practical flow performance. The pipe flows were well assessed using the developed Computational Fluid Dynamics model with effective rheological data integration, which is promising for practical design and optimisation of sewage sludge systems.

* Corresponding author at: P.O. Box 5048, 2600 GA Delft, the Netherlands.
E-mail address: P.Wei@tudelft.nl (P. Wei).

https://doi.org/10.1016/j.scitotenv.2021.145005

Nomenclature

A	A coefficient in the VTF model
CFD	Computational Fluid Dynamics
D	Pipe diameter, m
DGT	Digestate
E_a	Activation energy, $J \cdot mol^{-1}$
f	Fanning friction factor
K	Flow consistency index, $Pa \cdot s^n$
L	Pipe length, m
MR	Metzner and Reed
n, n'	Flow behaviour index, —
Q	Flow rate, kg/s
R	Gas constant, $J \cdot K^{-1} \cdot mol^{-1}$
$R1$	Electrical resistance, Ohm
Re	Reynolds number
RNG	*Re*-Normalisation Group
T	Temperature, °C and K
THP	Thermal-hydrolysis process
TS	Total solids
V	Mean pipe velocity, m/s
VTF	Vogel-Tammann-Fulcher
WAS	Waste activated sludge
WWTP	Wastewater treatment plant
X	A parameter in the Herschel-Bulkley-based *Re* expression

Greek symbols

α_0	Bingham infinite apparent viscosity, Pa·s
β	A parameter in the master curve equation
γ, $\dot{\gamma}$	Shear rate, s^{-1}
Γ	Normalised shear rate, —
ΔP	Pressure difference, Pa
μ_{eff_MR}	Effective dynamic viscosity, Pa·s
μ_T	Reference viscosity of the interstitial fluid, Pa·s
ρ	Density, kg/m^3
τ	Shear stress, Pa
τ_0	Yield stress, Pa
τ_W	Wall shear stress, Pa
T	Normalised shear stress, —
φ	A rheological parameter correlated by the VTF model

1. Introduction

Anaerobic digestion of municipal waste activated sludge (WAS), has been widely applied in wastewater treatment plants (WWTP). Sludge digestion targets both sludge mass reduction and the recovery of biochemical energy in the form of biogas. To enhance operational performance, compact installations for treating highly concentrated sludge matrices are promising and have been in focus (Jiang et al., 2014). Regarding total energy consumption, sludge pumping and mixing can use over 50% of the total energy demand in a WWTP (Kariyama et al., 2018; Kowalczyk et al., 2013). Cost-effective sludge pumping and mixing are hampered by the dynamic and highly viscous rheological behaviour of the WAS (Baudez et al., 2011; Jiang et al., 2014). Hence, to optimise process design and efficiency, proper assessment of the energy consumption for sludge pumping and mixing is of high importance (Eshtiaghi et al., 2012; Slatter, 2001), and relies on accurate sludge rheological characterisation.

Thus far, most researchers focused on describing the complex non-Newtonian behaviour in concentrated WAS with high total solids (TS) levels. Rheological properties of WAS have been found to have nonlinear relations to TS and temperature (Baudez, 2006; Baudez et al., 2011; Eshtiaghi et al., 2013; Markis et al., 2016; Ségalen et al., 2015a; Ségalen et al., 2015b; Seyssiecq et al., 2003). Additional rheological complexity results from thixotropic behaviour (Baudez and Coussot, 2001; Markis et al., 2016), which is defined as a reversible and time-dependent rheological change to specific shearing conditions imposed on a fluid (Seyssiecq et al., 2003). Moreover, some researchers focused on the application of rheological properties in sludge pumping systems and relevant pipe flows (Eshtiaghi et al., 2012; Proff and Lohmann, 1997; Slatter, 1997; Slatter, 2001), including pressure drop estimation (Farno et al., 2018; Proff and Lohmann, 1997). Although one study linking the sludge thixotropy to pumping energy estimation was published recently (Farno et al., 2020), quantitative correlations between flow behaviour and energy consumption are still limited. The aforementioned thixotropic behaviour (Baudez and Coussot, 2001; Markis et al., 2016) complicates the rheological characterisation using a single rheological model (Wei et al., 2018). In practice, this rheological variability or instability could be easily triggered by dynamic operational conditions, such as non-stabilised pumping processes, intermittent feeding/mixing modes and temperature fluctuations. Hence, clear characterisation of the complex and source-dependent rheology is still challenging. Consequently, the rheological-dependent correlations to flow and mixing behaviour has not been well developed, leading to limited application to process optimisation (i.e. energy consumption) in practice.

In this study, the complex rheological behaviour, especially thixotropy of WAS and anaerobic digestate (DGT) from the same WWTP, was investigated based on a long-term shearing condition. Variability to temperature was also combined to the complex rheological characterisation, with a view to potential changes of force interactions and equilibrium in the sludge matrix. Moreover, Computational Fluid Dynamics (CFD) simulations were performed to integrate the rheological properties into prediction and assessment of pipe flow and pressure drop.

2. Materials and methods

2.1. Sample characterisation

Sludge samples were taken from WWTP De Groote Lucht (Vlaardingen, the Netherlands), including WAS after gravitational thickening and DGT from the anaerobic digesters. So the samples could be representative to the sewage sludge in both transportation and digestion processes in the studied WWTP. WAS samples with higher TS concentrations were obtained using vacuum filtration to minimise changes in physical sludge structure. All the samples were stored at 4 °C and tested within four days. The solids content was measured using the standard methods (APHA, 2012).

2.2. Rheological measurements

Rheological properties were measured using an Anton Paar MCR 302 Rheometer (Anton Paar GmbH, Austria) equipped with a CC27 coaxial cylinder system (radius of the two concentric cylinders: 13.332 mm and 14.466 mm, respectively). Measurements, including flow curve and yield stress, were carried out based on the proposed methods from our previous work (Wei et al., 2018).

2.2.1. Flow curve

(1) After reaching a stabilised set temperature (tolerance ±0.05 °C), the sample was pre-sheared (16.7 s^{-1}) for 90 s, to minimise concentration gradients achieving a homogeneous distribution; (2) followed by a rest of 60 s; (3) a flow measurement in a logarithmical ramp mode, with an applied shear rate range of 0.01– 1000 s^{-1}. For studying the long-term shearing impact, step (3) was successively repeated in six rounds at 20 °C to the same sample. For studying the temperature impact, five temperatures were applied that cover a wide range of operational conditions (transport, heat exchange, digestion), including 10, 20, 35, 45 and 55 °C.

2.2.2. Yield stress

The same procedure was used as with (1) and (2); (3) a measurement in a torque ramp mode, starting from a low torque level with a gradual increase to capture the yielding process with a critical change of the monitored deflection angle.

Except the long-term shearing scenario (one-time measurement), triplicate measurements were normally implemented, and good data consistency with small overall standard deviation (≤4%) was obtained. So rheological data of the long-term shearing could be representative to the WAS with the given TS concentration.

2.3. Hydrodynamics and energy assessment

A CFD model for flows in a circular pipe was developed based on the sludge pipeline system operated in the aforementioned WWTP, of which the diameter is 20 cm. The preliminary 3D results showed axisymmetric velocity profiles so finally a 2D axisymmetric assumption was applied. A length/diameter (L/D) ratio of 40 was set to ensure generation of fully-developed flows. Physical properties of fluid were specified using the measured data of WAS and DGT. Pressure-driven flows, assuming a fixed pressure gradient along the horizontal pipe, were simulated in both laminar and turbulent cases. The *Re*-Normalisation Group (RNG) k-ε model was used for turbulence, which supports the simulation of turbulent flows with relatively low Reynolds number (*Re*) values. Model reliability was first determined by a grid independency study, and a domain with optimal mesh dimensions (characteristic resolution 0.004 m) was selected for the following simulations. In each case, a converged fully-developed flow was determined not only by low residuals ($<10^{-5}$), but also by a force balance (imbalanced force ratio < 5%) between wall shear stress and pressure-driven force. Simulations were carried out using the commercial package ANSYS-Fluent 17.1 on a Dell Optiplex 7010 computer, with Intel Core i5–3740 and 8 GB RAM.

A non-Newtonian pipe flow can be characterised using a generalised *Re* (Metzner and Reed, 1955)

$$Re_{MR} = \frac{\rho V D}{\mu_{eff\_MR}}, \tag{1}$$

where ρ is fluid density; V is mean pipe flow velocity; D is pipe diameter; and μ_{eff_MR} is effective dynamic viscosity depending on applied rheological models. For Ostwald (or power-law) model, the apparent viscosity μ and the Re_{MR} in laminar flow regime (Metzner and Reed, 1955) are expressed as

$$\mu = K\gamma^{n-1}, \tag{2}$$

$$Re_{MR} = \frac{\rho V D}{K\left(\frac{8V}{D}\right)^{n-1}\left(\frac{3n+1}{4n}\right)^{n}}, \tag{3}$$

where γ is shear rate; and K and n are the fluid consistency coefficient and the flow behaviour index, respectively. For Herschel-Bulkley model, the μ and Re_{MR} (Chilton and Stainsby, 1998) are expressed as

$$\mu = \frac{\tau_0}{\gamma} + K\gamma^{n-1}, \tag{4}$$

$$\begin{cases} Re_{MR} = \dfrac{\rho V D}{K\left(\frac{8V}{D}\right)^{n-1}\left(\frac{3n+1}{4n}\right)^{n}\left(\frac{1}{1-X}\right)\left(\frac{1}{1-aX-bX^2-cX^3}\right)^{n}} \\ X = \dfrac{\tau_0}{\tau_W} = \dfrac{4L\tau_0}{D\Delta P}, a = \dfrac{1}{2n+1}, b = \dfrac{2n}{(n+1)(2n+1)}, c = \dfrac{2n^2}{(n+1)(2n+1)} \end{cases}, \tag{5}$$

where τ_0 is yield stress; L is pipe length; ΔP is pressure difference; and τ_W is wall shear stress. Pressure drop in pipe flows can be estimated as:

$$\frac{\Delta P}{L} = \frac{4f}{D}\cdot\frac{\rho V^2}{2}, \tag{6}$$

where f is the Fanning friction factor. For laminar flows f is expressed as

$$f = \frac{16}{Re_{MR}}. \tag{7}$$

For turbulent flows, f is modified as (Dodge and Metzner, 1959):

$$\frac{1}{\sqrt{f}} = \frac{4}{n'^{0.75}}\log\left(Re_{MR} f^{\frac{2-n'}{2}}\right) - \frac{0.4}{n'^{1.2}}, \tag{8}$$

where n' is another flow behaviour index and usually has the same value as n. It should be noted that regarding laminar pipe flows of a non-Newtonian fluid characterised by Ostwald model, Eq. (3) is used to calculate the pressure drop (Metzner and Reed, 1955):

$$\frac{\Delta P}{L} = \frac{4}{D}K\left(\frac{3n+1}{4n}\right)^{n}\left(\frac{8V}{D}\right)^{n}. \tag{9}$$

3. Results and discussion

3.1. Characterisation of time-dependent rheological properties by long-term shearing

Rheological impact of long-term shearing was characterised by the six rounds of flow curve measurements, for both DGT and WAS samples. As shown in Fig. 1A, for the DGT sample with a TS concentration of 2.6% (further referred to DGT 2.6%), similar flow curves were obtained for each round. On the contrary, Fig. 1B showed a considerable decrease in shear stress over the shear rate range of the WAS sample with a TS concentration of 6.7% (further referred to WAS 6.7%). The change in shear stress decreased as the rounds were repeated, and almost superposed flow curves were obtained after Round 4. Similarities were also found in the yield stress measurements. As depicted in Fig. 1C, yield stress data of all the samples shows an asymptotic tendency, indicating that stabilised rheological properties were achieved under the long-term shearing condition. Hence, besides the initial state in Round 1, another rheological state in Round 6 was determined. From here on, these states are referred to as 'Initial' and 'Stable' state, respectively. This means that at a specific shear rate, the maximum and minimum apparent viscosity of a sample was determined by the Initial and Stable state, respectively. Thus, any time-dependent variation in apparent viscosity would range in this determined range, regardless shearing duration.

Several models were applied to characterise the Initial and Stable flow curves, including Ostwald, Herschel-Bulkley, a modified model developed by Baudez et al. (2011), and the hybrid model proposed in our previous study (Wei et al., 2018). For the WAS curves, Ostwald and Herschel-Bulkley failed to obtain a good fitting. The modified model performance was not satisfactory, despite prior successful reports in a wide range of shear rates (Baudez et al., 2011; Baudez et al., 2013b; Ségalen et al., 2015b). Similar to our previous study (Wei et al., 2018), the hybrid model fitting was the best, in which Herschel-Bulkley fitted the low and medium shear rates, and Ostwald fitted the high shear rates (detailed fitted shear rates are shown in Table S1). For the DGT samples, Herschel-Bulkley achieved good fitting performance for the whole curves. As shown in Table S1, large differences were found for WAS: all shear stress values were reduced by about 50% from Initial to Stable. In combination with the considerable changes of K and n, Initial and Stable states demonstrated distinct rheological behaviour. For DGT, the differences in the rheological parameters between Initial and Stable were much lower than for WAS sludge.

The reduced yield stress and K values implied unsteady restructuring of the sludge, in which the viscoelasticity, accounting for both viscous

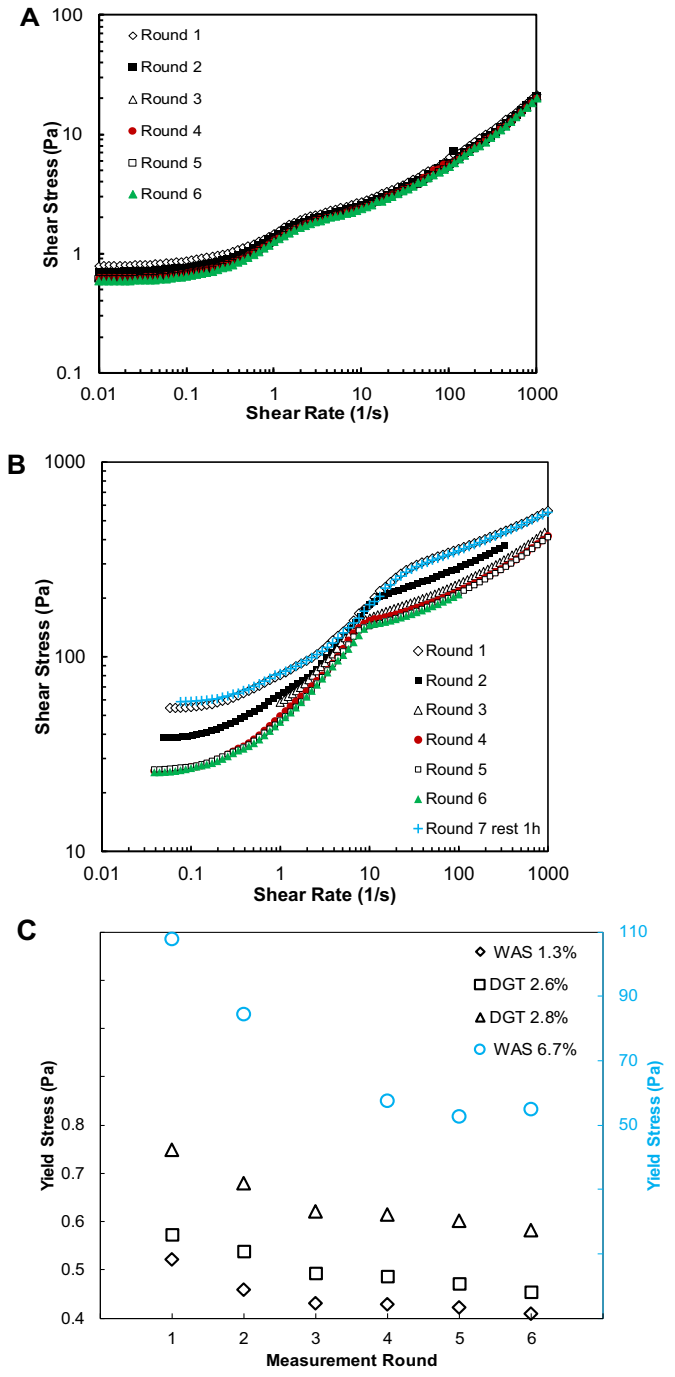

Fig. 1. Rheological data measured in 6 rounds, flow curves of A: DGT, TS 2.6%; B: WAS, TS 6.7%; and C: variation of yield stress.

and elastic behaviour, became weakened under the long-term shearing condition. This structural change could eventually lead to a shift of equilibrium between the particles' colloidal forces (non-hydrodynamic) and hydrodynamic forces (Baudez, 2008), which was reflected by reaching another stabilised rheological state after the long-term shearing. The structural/rheological evolution, that was characterised by two critical transitions (Table S1), has some similarity to previous reported studies (Baudez, 2008; Baudez et al., 2011), but reveals a different pattern. The Stable curve differed completely from the Initial curve, however, rheology changed back to nearly its Initial state after a resting period of about 1 h, indicating reversible structural deformation. In summary, shearing history had a strong and reversible impact on WAS, while the impact on DGT sludge was small. Considering that both WAS and DGT originated from the same WWTP, the obtained results also indicated that the thixotropic behaviour of the sludge was distinctly weakened during the digestion process.

3.2. Temperature impact on rheology: role of solids content

Since the studied temperature change was modest and all measurements were done in a relatively short time (~20 min), occurrence of any thermal-treatment/aging process of the samples was negligible. Hence, relevant changes of sludge composition and solubilisation reported in some studies (Farno et al., 2015) were not considered or discussed in this study. Fig. 2A and B show the Initial (Round 1) flow curves of DGT 3.1% and WAS 7.0% at five temperatures. In both cases, shear stress decreased as temperature increased, while curve profiles were similar in the whole shear rate range. However, yield stress data show different

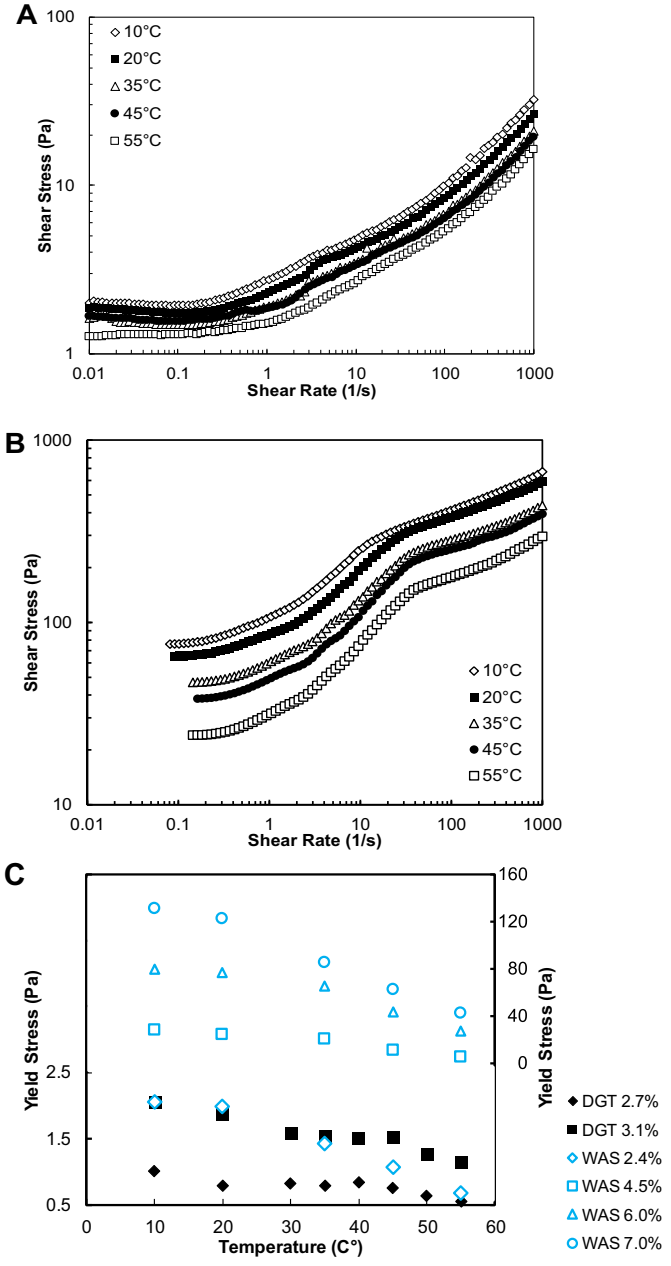

Fig. 2. Rheological data at different temperatures, flow curves of A: DGT 3.1%; B: WAS 7.0%; and C: yield stress of DGT and WAS.

trends between the two sludge types (Fig. 2C): WAS has a monotonic decrease, while DGT has a plateau region. An almost constant yield stress was obtained from 30 °C to 45 °C, bridging the two decrease regions of 10 °C ~ 20 °C, and 45 °C ~ 55 °C. This similarity was also observed in the almost overlapped flow curves of 35 °C and 45 °C (Fig. 2A), and it agrees with a previously reported study of digested sludge, in which a considerable decrease in yield stress was only observed at temperatures over 40 °C (Baudez et al., 2013b). These results indicate an insensitive impact on yield stress when the temperature varied within the range of commonly applied mesophilic digestion temperatures, i.e. 35 ± 5 °C, at which the anaerobic digester was operated at full scale. WAS rheology revealed a higher sensitivity towards temperature changes, since the yield stress value started to plunge over 20 °C.

Several models have been reported to have a good correlation between temperature and rheological properties, including an exponential relation (Manoliadis and Bishop, 1984), the Arrhenius model (Baroutian et al., 2013), and the Vogel-Tammann-Fulcher (VTF) model (Baudez et al., 2013a; Dieudé-Fauvel et al., 2009; Ségalen et al., 2015b). The VTF model is expressed as,

$$\varphi = A \cdot \exp\left(\frac{E_a}{R} \cdot \frac{1}{T - T_0}\right), \tag{10}$$

where A is a model coefficient, E_a is activation energy, R is the gas constant, and T_0 is a critical temperature for vitreous, or glassy transition.

The VTF model has been successfully applied for the non-hydrodynamic dominant regime of sludge with a medium TS level (<5%) (Baudez et al., 2013a; Baudez et al., 2013b) and pasty sludge with a high TS level (>10%) (Dieudé-Fauvel et al., 2009; Ségalen et al., 2015b). In this study, it was also found to have the best fit of all WAS yield stress (τ_0) data. However, different temperature correlations were found with other model parameters. For WAS 4.5% (Fig. 3A), similar to τ_0, $K2$ and τ_1 decreased following the VTF model; whereas the $K1$ decreasing trend was best fit by the exponential relation. As temperature increased, $n1$ increased while $n2$ had no considerable change. Similarities were obtained in the other concentrated WAS with TS concentrations >2.5%, which are not shown here. The obtained results implied shear rate dependency on the aforementioned structural deformation and the changes of force interactions in WAS. At low and medium shear rates (segment 1), a good Arrhenius correlation was obtained between $K1$ and the water dynamic viscosity (Fig. 3B). The increased $n1$ indicates a lower degree of shear-thinning, a higher degree of fluidity, and also a higher degree of electrical conductivity status (Ségalen et al., 2015b). Hence, changes in the hydrodynamic interactions affected by temperature were apparently more reflected at low shear rates. At high shear rates, the VTF model better fitted $K2$, which reflected the impact of sludge solids content, and thus implied a more dominant influence of the non-hydrodynamic interactions. However, the negligible $n2$ change indicated the shear-thinning degree was almost independent on temperature at high shear rates, which agrees with reported results (Baroutian et al., 2013; Manoliadis and Bishop, 1984).

The rheological impact of temperature was also strongly correlated to the solids content level. Unlike the fitting results for the more concentrated WAS, both Herschel-Bulkley and the modified model (Baudez et al., 2011) had acceptable fitting performance at TS < 2.5%. For the model derived yield stress, a good correlation with the VTF model was obtained. As shown in Fig. 3B (the blue data), the Bingham infinite viscosity α_0 has a good linear relation with the water dynamic viscosity, indicating a good Arrhenius correlation and considerable hydrodynamic interactions over the entire shear rate range. Apparently, these results agree quite well with the previous studies (Baudez et al., 2013b; Dieudé-Fauvel et al., 2009; Ségalen et al., 2015b). However, good temperature correlations to K and n were difficult to achieve with any of the aforementioned models. The VTF model performance was found

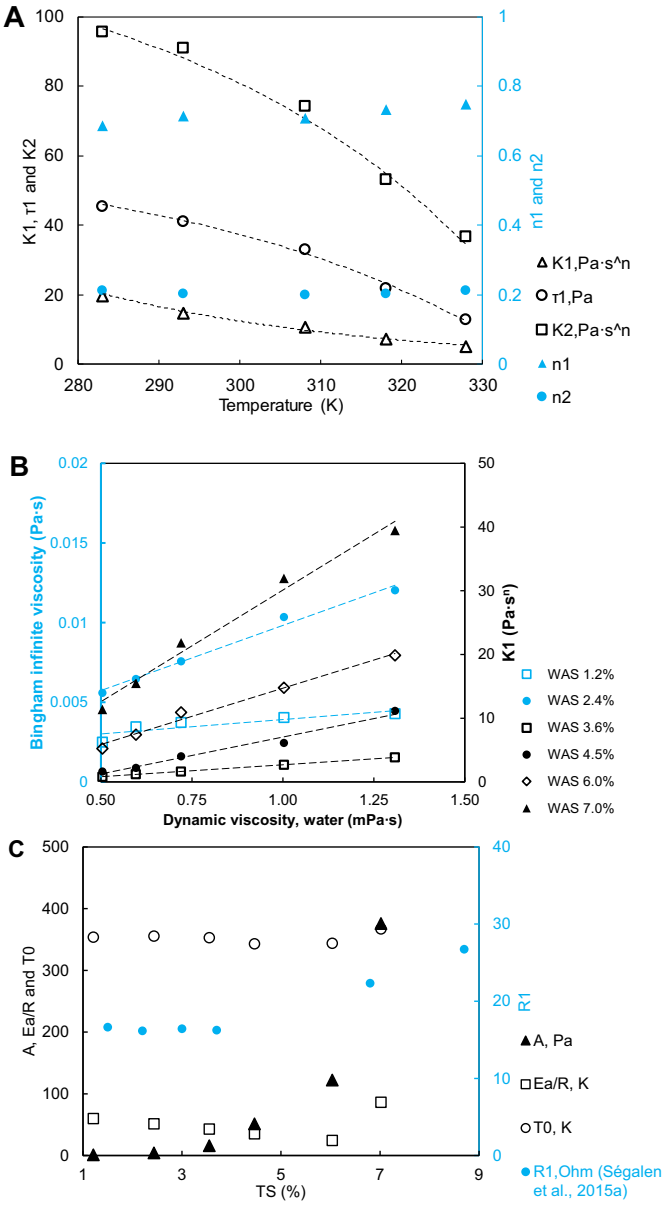

Fig. 3. Model correlation results. A: To temperature, WAS 4.5%; B: to water dynamic viscosity, all WAS samples; and C: the VTF model parameters for τ_0 to TS concentration, compared to experimental data (Ségalen et al., 2015a).

to be more correlated to the TS level. Comparable values of the regressed E_a and T_0 (in Eq. (10)) in τ_0, $K2$ and τ_1 correlations were only found in a TS range between 2.5% and 6%. However, a large deviation was found between E_a and T_0 when TS < 2.5% and TS > 6%. As reported by Dieudé-Fauvel et al. (2009), it indicates similar patterns of involved molecular movements and particle interactions, mainly occurring in a specific TS range.

Fig. 3C shows the fitting results of the VTF model for τ_0 at different TS concentrations. All of the three parameters, especially E_a and A (related to activation intensity), have a distinct increase at TS > 6%. It has been reported that the rheological properties also correlate well to sludge electrical properties (Dieudé-Fauvel et al., 2009; Ségalen et al., 2015a; Ségalen et al., 2015b), which can be characterised by same activation energy (E_a) results between apparent viscosity and electrical resistivity (Dieudé-Fauvel et al., 2009). In their developed equivalent circuit model, an electrical resistance $R1$ was defined to represent the interactions and network of solid compounds (the non-hydrodynamic

discussed in our study) (Ségalen et al., 2015a; Ségalen et al., 2015b), which was also shown in Fig. 3C. The *R1* variation, a slight initial decrease and a critical increase in the range between 3.7% and 6.8% TS (Ségalen et al., 2015a), has a similar trend to our results. Hence, increasing solids content over a threshold may lead to a critical change or evolution of the non-hydrodynamic interaction intensity, illustrated by the considerable rheological changes in Fig. 3C.

Moreover, the interactive impacts between temperature and solids content on sludge rheology may change through aging processes. After long-term mesophilic digestion, solids content of digestate can be stabilised (almost constant TS and VS concentrations), which is characterised by similar non-hydrodynamic interactions over a wider temperature range of 30– 40 °C. This may clarify the aforementioned insensitivity of DGT yield stress change to temperature (Fig. 2C).

3.3. Further discussion: implication of dynamic structural change

Similarity of rheological behaviour under different conditions can be determined by dimensionless master curves (Baudez and Coussot, 2001; Baudez et al., 2011; Coussot, 1995). As mentioned before, the DGT flow curves showed a good fit over the whole shear rate range, justifying the use of the following equation (Baudez et al., 2011)

$$\begin{cases} T_M = 1 + \beta \cdot \Gamma_A^{\,n} + \Gamma_A \\ T_M = \dfrac{\tau}{\tau_0}, \Gamma_A = \dfrac{\alpha_0}{\tau_0} \cdot \dot{\gamma}, \beta = \dfrac{K}{\tau_0} \cdot \left(\dfrac{\tau_0}{\alpha_0}\right)^n \end{cases}, \quad (11)$$

where α_0 is the Bingham infinite apparent viscosity (Pa·s). For WAS curves, since the modified model (Baudez et al., 2011) was no longer appropriate, another equation with a reference viscosity (Baudez and Coussot, 2001; Coussot, 1995) was used

$$\begin{cases} T_M = 1 + \lambda \cdot \Gamma_B^{\,n} \\ T_M = \dfrac{\tau}{\tau_0}, \Gamma_B = \dfrac{\mu_T}{\tau_0} \cdot \dot{\gamma}, \lambda = \dfrac{K}{\tau_0} \cdot \left(\dfrac{\tau_0}{\mu_T}\right)^n \end{cases}, \quad (12)$$

where μ_T is the reference viscosity of the interstitial fluid (water). It was found that the curve trend was independent on μ_T. For the sake of simplicity, the μ_T value was set to 1 at 20 °C, and varied accordingly with the change in water dynamic viscosity at other temperatures.

As shown in Fig. 4A, all DGT curves were very close to form one master curve. In line with the previous results (Baudez et al., 2011; Ségalen et al., 2015b), it implied similar hydrodynamic and non-hydrodynamic interactions in DGT within the studied temperature and TS ranges. The aforementioned weak thixotropic behaviour was only reflected by the small deviation between the Initial and Stable curves when $\Gamma > 2$. However, for WAS, distinct curves were obtained between 10 °C and 55 °C, with a marked change at around $\Gamma = 0.2$. Unlike the DGT results, the WAS Initial and Stable curves started to separate when $\Gamma > 0.1$, and the difference kept increasing when $\Gamma > 1$. Moreover, separated curves of 10 °C and 55 °C were also observed in the other concentrated WAS (TS > 2.5%). Hence, a single master curve was only formed in DGT and WAS with low TS concentrations (< 2.5%), but not for the other concentrated WAS, which was, to the authors' knowledge, never reported in previous research.

However, larger scaled shear stress (T_M) values in Initial 55 °C and Stable 20 °C curves could be noticed. These indicated a higher viscous or less flowable degree, which was unexpected and is seemingly contradictory to the original data shown in Figs. 1 and 2. In Eq. (12), T_M also represents the relative shear stress to the referred τ_0. When comparing the Initial 10 °C and 55 °C curves, the trend illustrated variations in the relative shear stress from low to high shear rates, which might be related to dynamic behaviour of the force interactions in WAS. As discussed in Section 3.2, the hydrodynamic interactions could be considerable at low shear rates, similarly to DGT, the two curves were close to each other. As reported in our previous study (Wei et al.,

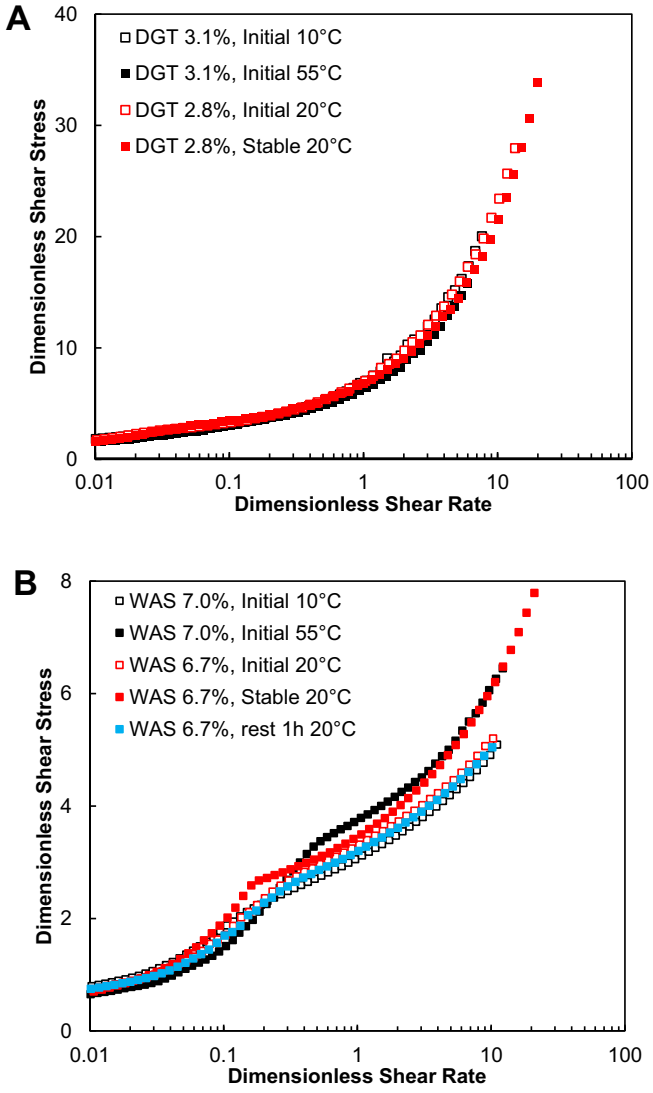

Fig. 4. Dimensionless flow curves of A: DGT samples, and B: WAS samples.

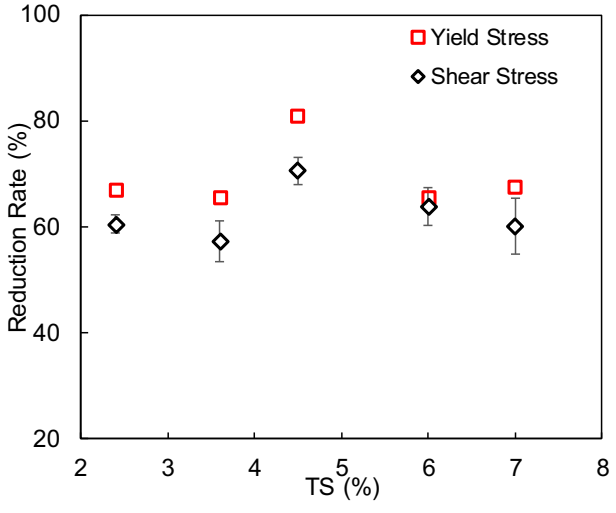

Fig. 5. Mean reduction rates (between 10 °C and 55 °C) of yield stress and shear stress in flow curves (>5 s^{-1}) at different TS concentrations of WAS.

2018), localised shear (Baudez et al., 2011) could occur, as demonstrated by the part of the curve where shear stress was lower than τ_0. As temperature increased, localised shear could be mitigated, which means that WAS became more flowable, leading to lower T_M at 55 °C than at 10 °C. However, as shear rate increased, collision and interaction probability of the particles increased, and more energy was dissipated for particle dispersion (Coussot, 1995; Tsutsumi and Yoshida, 1987). Therefore, in Section 3.2 the non-hydrodynamic interactions could become more important at high shear rates. Due to the changes of the hydrodynamic and non-hydrodynamic interactions, the relevant force equilibrium to maintain sludge rheological behaviour would be dynamic and shifting. As shown in Fig. 5, the mean shear stress reduction in the flow curves is systematically lower than yield stress reduction. It indicated that, after yielding, the generated destruction degree of sludge structure was not constant, but became less and towards a more structural reconstruction state at higher temperatures and higher shear rates, resulting in higher T_M values at 55 °C than at 10 °C. Similarities were also found between Initial 20 °C and Stable 20 °C: yield stress was reduced by 51.0% while the mean shear stress was reduced by only 33.1 ± 7.7%.

Moreover, trend differences in the curves between temperature increase (Initial 10 °C and 55 °C) and shearing time change (Initial and Stable 20 °C) also implied different mechanisms of shifting the force equilibrium. The Initial 10 °C and 55 °C curves in Fig. 4B are almost parallel after the cross point at $\Gamma = 0.2$. The parallel trend implied that the equilibrium shift and the destruction degree change due to temperature were independent of the shear rate, consistent with the results of decreasing *K2* and constant *n2* shown in Section 3.2. Hence, temperature apparently mainly affected the intensity of the overall hydrodynamic and non-hydrodynamic interactions, but not the pattern and related structure of flocs and agglomerated particles. However, no parallel trend could be observed in Initial and Stable 20 °C curves. Since the hydrodynamic interactions were consistent at the same temperature, the long-term shearing effect on the equilibrium shift appears to be related to the non-hydrodynamic interactions. On one hand, the decrease in transition shear rate (Table S1) indicated less and less localised shear, implying that long-term shearing led to much weaker attractive forces between the flocs and agglomerated particles, and a higher destruction degree. On the other hand, the consequent characteristic size reduction was accompanied by an increased number of these solids content. This caused the collision and interactive probability to increase along with the shear rate, leading to a T_M trend no longer parallel to that for Initial (Fig. 4B). Hence, the long-term shearing apparently affected both the intensity and pattern of the non-hydrodynamic interactions, and eventually resulted in reaching another force equilibrium determined as Stable in this study. The microscopic force and structural changes between Initial and Stable states could be macroscopically demonstrated by the considerable changes of rheological parameters, including *K*, *n* and T_M. In addition, these changes seem reversible since the curve fell back to Initial after a long-time rest.

Hence, essentially this T_M deviation had no contradiction to the original data and referred studies. It supported the theoretical interpretation in literature (Baudez et al., 2011; Coussot, 1995; Tsutsumi and Yoshida, 1987) and implied different mechanisms of shifting the force equilibrium between the long-term shearing and temperature impacts.

3.4. Application of the rheological discrepancy: pipe flow assessment

For both WAS and DGT, flow behaviour of Initial and Stable states was investigated using CFD models. Model validity was first determined using reference data, including Newtonian (water, 20 °C) and non-Newtonian (Pinho and Whitelaw, 1990) pipe flows. As shown in Fig. S1, a good agreement was achieved between the referred data and simulation results. However, unlike Newtonian, the non-Newtonian velocity profiles showed a higher rheological dependency.

As shown in Fig. S2 and Table S3, the aforementioned rheological discrepancy between Initial and Stable was clearly demonstrated in the hydrodynamic data, especially for WAS. In addition, the difference between Initial and Stable increases as the pressure gradient (Pa/m) decreases. Therefore, it implies a considerable change of flow behaviour when the sludge, especially the WAS, frequently changes between Initial and Stable states under a specific pumping or mixing condition.

Although an optimal rheological characterisation was achieved, the hybrid model did not lead to a satisfactory energy assessment of the WAS pipe flows. In Re_{MR} calculation, the involved sub-models: Herschel-Bulkley and Ostwald with distinct K and n values, could not be well integrated and had to be applied individually. As shown in Table 1, different Re_{MR} values were obtained between the sub-models, indicating that both governed shear rate segments played an important role in the flow characteristics. In order to improve flow characterisation, an 'effective' Ostwald model was applied, and the parameters K_{eff} and n_{eff} were not determined by the experimental data fitting but by regression of Eq. (9) (Metzner and Reed, 1955). As expected, it could predict more reasonable Re_{MR} with moderate values (Table 1) compared to the two sub-models. The effective model was further validated using the Moody diagram. As shown in Fig. 6, the WAS data have a good correlation to the Hagen-Poiseuille line, representing the theoretical relation between the Fanning friction factor and *Re* in the laminar regime (typically $Re < 2100$). A good correlation was also obtained for the DGT data in both the laminar regime and the turbulent regime determined by a modified expression (Eq. (8), (Dodge and Metzner, 1959)).

Fig. 7 shows pressure drop variations in the studied flow rate range, based on a developed correlation from a more practical aspect (Metzner and Reed, 1955)

$$\frac{\Delta P}{L} = 32K\frac{8^{n'-1}}{D^{3n'+1}}\left(\frac{3n+1}{4n}\right)^{n}\left(\frac{4Q}{\pi}\right)^{n'}, \tag{13}$$

where *Q* is flow rate. Limitation of the single sub-model use was also illustrated in the correlation performance (Fig. 7A): hybrid Herschel-

Table 1
Re_{MR} of WAS and DGT predicted by different models.

	WAS 6.7%				DGT 2.6%	
	Effective *dP/L* (Pa/m)	Re_{MR}, Hybrid Herschel-Bulkley	Re_{MR}, Hybrid Ostwald	Re_{MR}, 'Effective' Ostwald	Effective *dP/L* (Pa/m)	Re_{MR}, Herschel-Bulkley
Initial	2.5E+3	0.3	0.2	0.2	67	7.2E+2
	5.0E+3	4.5	3.9	4.2	84	1.3E+3
	8.4E+3	90	175	157	134	3.6E+3
	1.1E+4	435	1346	1085	240	1.0E+4
					466	2.7E+4
					1135	9.8E+4
Stable	2.5E+3	1.3	1.0	1.4	60	1.0E+3
	4.6E+3	46	167	142	88	1.7E+3
	5.4E+3	148	912	666	130	4.6E+3
	8.3E+3	341	2945	1934	242	1.2E+4
					470	3.2E+4
					1125	1.1E+5

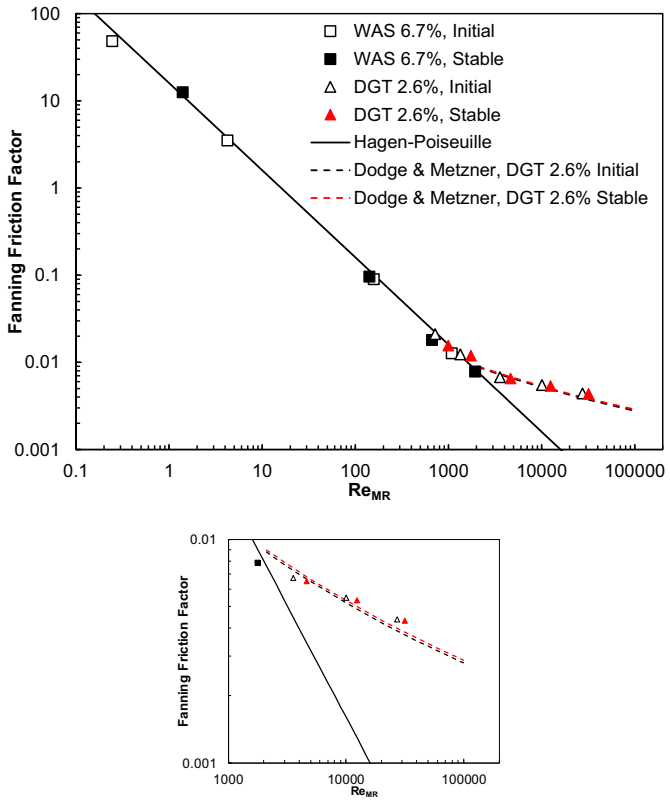

Fig. 6. Moody diagram of Initial and Stable of WAS (the 'effective' Ostwald model) and DGT.

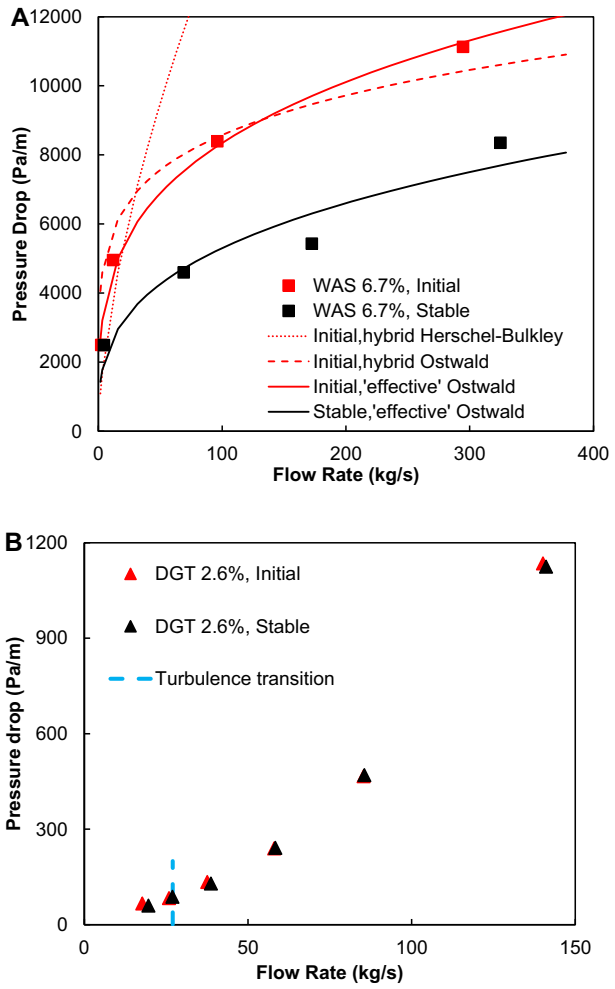

Fig. 7. Correlations of the pressure drop to the flow rates, A: WAS, and B: DGT.

Bulkley was only valid at very low flow rates before getting large deviations; hybrid Ostwald had a considerable underestimation at high flow rates. However, the 'effective' Ostwald model got good correlations for both Initial and Stable states. It again emphasised the importance of determining K_{eff} and n_{eff}, and the considerable pressure drop reduction (> 33%) from Initial to Stable. Correlating to the rheological changes between Initial and Stable, some quantitative solutions were proposed to assess general time-dependent laminar pipe-flow behaviour of the WAS. A range of pressure drop could be determined based on Initial and Stable state, expressed as

$$\frac{\Delta P}{L} = \begin{cases} 1838 \cdot \frac{1.54^{0.32}}{D^{1.95} \cdot 8^{0.68}} \cdot \left(\frac{4Q}{\pi}\right)^{0.32}, \min\ (by\ Stable) \\ 3501 \cdot \frac{1.66^{0.28}}{D^{1.83} \cdot 8^{0.72}} \cdot \left(\frac{4Q}{\pi}\right)^{0.28}, \max\ (by\ Initial) \end{cases} \quad (14)$$

Thus, at a specific flow rate, the corresponding pressure drop is expected to vary within the determined range. This is especially useful for achieving an optimised operation for sludge pumping, i.e. in sludge systems with a high and low temperature thermal-hydrolysis process (THP) as pre-treatment. In these systems, the transport of highly concentrated sludge mixtures and the batch-wise feeding of certain THP configurations leads to high pumping energy consumption, non-optimised heat transfer and even clogging. Switching off or even reducing pumping/mixing power for some time should therefore be considered due to the reversible thixotropic behaviour. After a rest period, the dynamic force equilibrium would shift and reconstruction to Initial could occur, increasing the stagnant and poor flow regions. The installed pump/mixer capacity should be designed to handle the Initial rheology, in order to trigger the sludge motion again.

Furthermore, it should be noticed that K_{eff} and n_{eff} were mainly developed to characterise flow behaviour under specific flow conditions, i.e., a flow rate/pressure gradient range, which is more related to practical applications such as pump design. For thixotropic materials, it is not easy to determine K_{eff} and n_{eff}, because they are not explicitly derived from the rheogram, which may require systematic experiments or simulations. More attention is also required to the last WAS group and the second DGT group (Fig. 7B), since the Re_{MR} values were close to the aforementioned critical value (around 2100) for turbulence transition. If the imposed pressure gradient increased further, turbulence may occur, which will lead to a considerable increase in pressure drop and thereby might complicate practical operations. Hence, the integration of experimental and CFD approaches developed in this study sheds light on a better solution to the aforementioned issues in practice.

4. Conclusions

- The complex thixotropic behaviour of the studied sewage sludge was well characterised by the two quantified limitation states: Initial and Stable.
- Impact discrepancy between the long-term shearing and temperature, implied different mechanisms to shift the equilibrium of hydrodynamic and non-hydrodynamic interactions for structure deformation and recovery.
- The distinct rheological properties between Initial and Stable were clearly reflected in pipe flow behaviour, revealing a concrete link between lab-measured sludge rheology and its practical flow performance.

- The pipe flows with complex rheological properties were well assessed using the developed CFD model with effective rheological data integration, which is promising for practical design and optimisation of sewage sludge systems.

CRediT authorship contribution statement

Peng Wei: Conceptualization, Methodology, Software, Validation, Formal analysis, Investigation, Writing – original draft. **Wim Uijttewaal:** Methodology, Writing – review & editing, Supervision. **Jules B. van Lier:** Writing – review & editing, Supervision. **Merle de Kreuk:** Conceptualization, Methodology, Writing – review & editing, Supervision.

Declaration of competing interest

The authors declare that they have no known competing financial interests or personal relationships that could have appeared to influence the work reported in this paper.

Acknowledgements

The authors appreciate the collaborations with Ir. Mark van den Braak from De Groote Lucht WWTP (Vlaardingen, the Netherlands); and MSc. Qiuman Tan for rheological measurements. China Scholarship Council and Lamminga Fonds are acknowledged to support Peng Wei's research at Delft University of Technology.

Appendix A. Supplementary data

Supplementary data to this article can be found online at https://doi.org/10.1016/j.scitotenv.2021.145005.

References

APHA, 2012. Standard Methods for the Examination of Water and Wastewater. 22nd edition. American Public Health Association, American Water Works Association, Water Environment Federation, Washington.

Baroutian, S., Eshtiaghi, N., Gapes, D.J., 2013. Rheology of a primary and secondary sewage sludge mixture: dependency on temperature and solid concentration. Bioresour. Technol. 140, 227–233.

Baudez, J.-C., 2006. About peak and loop in sludge rheograms. J. Environ. Manag. 78, 232–239.

Baudez, J.C., 2008. Physical aging and thixotropy in sludge rheology. Appl. Rheol. 18, 8.

Baudez, J.C., Coussot, P., 2001. Rheology of aging, concentrated, polymeric suspensions: application to pasty sewage sludges. J. Rheol. 45, 1123–1139.

Baudez, J.C., Markis, F., Eshtiaghi, N., Slatter, P., 2011. The rheological behaviour of anaerobic digested sludge. Water Res. 45, 5675–5680.

Baudez, J.-C., Gupta, R.K., Eshtiaghi, N., Slatter, P., 2013a. The viscoelastic behaviour of raw and anaerobic digested sludge: strong similarities with soft-glassy materials. Water Res. 47, 173–180.

Baudez, J.C., Slatter, P., Eshtiaghi, N., 2013b. The impact of temperature on the rheological behaviour of anaerobic digested sludge. Chem. Eng. J. 215-216, 182–187.

Chilton, R.A., Stainsby, R., 1998. Pressure loss equations for laminar and turbulent non-Newtonian pipe flow. J. Hydraul. Eng. 124, 522–529.

Coussot, P., 1995. Structural similarity and transition from Newtonian to non-Newtonian behavior for clay-water suspensions. Phys. Rev. Lett. 74, 3971–3974.

Dieudé-Fauvel, E., Van Damme, H., Baudez, J.C., 2009. Improving rheological sludge characterization with electrical measurements. Chem. Eng. Res. Des. 87, 982–986.

Dodge, D.W., Metzner, A.B., 1959. Turbulent flow of non-newtonian systems. AIChE J. 5, 189–204.

Eshtiaghi, N., Markis, F., Slatter, P., 2012. The laminar/turbulent transition in a sludge pipeline. Water Sci. Technol. 65, 697–702.

Eshtiaghi, N., Markis, F., Yap, S.D., Baudez, J.-C., Slatter, P., 2013. Rheological characterisation of municipal sludge: a review. Water Res. 47, 5493–5510.

Farno, E., Baudez, J.C., Parthasarathy, R., Eshtiaghi, N., 2015. Impact of temperature and duration of thermal treatment on different concentrations of anaerobic digested sludge: kinetic similarity of organic matter solubilisation and sludge rheology. Chem. Eng. J. 273, 534–542.

Farno, E., Coventry, K., Slatter, P., Eshtiaghi, N., 2018. Role of regression analysis and variation of rheological data in calculation of pressure drop for sludge pipelines. Water Res. 137, 1–8.

Farno, E., Lester, D.R., Eshtiaghi, N., 2020. Constitutive modelling and pipeline flow of thixotropic viscoplastic wastewater sludge. Water Res. 184, 116126.

Jiang, J., Wu, J., Poncin, S., Li, H.Z., 2014. Rheological characteristics of highly concentrated anaerobic digested sludge. Biochem. Eng. J. 86, 57–61.

Kariyama, I.D., Zhai, X., Wu, B., 2018. Influence of mixing on anaerobic digestion efficiency in stirred tank digesters: a review. Water Res. 143, 503–517.

Kowalczyk, A., Harnisch, E., Schwede, S., Gerber, M., Span, R., 2013. Different mixing modes for biogas plants using energy crops. Appl. Energy 112, 465–472.

Manoliadis, O., Bishop, P.L., 1984. Temperature effect on rheology of sludges. Journal of Environmental Engineering-Asce 110, 286–290.

Markis, F., Baudez, J.-C., Parthasarathy, R., Slatter, P., Eshtiaghi, N., 2016. The apparent viscosity and yield stress of mixtures of primary and secondary sludge: impact of volume fraction of secondary sludge and total solids concentration. Chem. Eng. J. 288, 577–587.

Metzner, A.B., Reed, J.C., 1955. Flow of non-newtonian fluids—correlation of the laminar, transition, and turbulent-flow regions. AIChE J. 1, 434–440.

Pinho, F.T., Whitelaw, J.H., 1990. Flow of non-newtonian fluids in a pipe. J. Non-Newtonian Fluid Mech. 34, 129–144.

Proff, E.A., Lohmann, J.H., 1997. Calculation of pressure drop in the tube flow of sewage sludges with the aid of flow curves. Water Sci. Technol. 36, 27–32.

Ségalen, C., Dieudé-Fauvel, E., Baudez, J.C., 2015a. Electrical and rheological properties of sewage sludge – impact of the solid content. Water Res. 82, 25–36.

Ségalen, C., Dieudé-Fauvel, E., Clément, J., Baudez, J.C., 2015b. Relationship between electrical and rheological properties of sewage sludge – impact of temperature. Water Res. 73, 1–8.

Seyssiecq, I., Ferrasse, J.-H., Roche, N., 2003. State-of-the-art: rheological characterisation of wastewater treatment sludge. Biochem. Eng. J. 16, 41–56.

Slatter, P.T., 1997. The rheological characterisation of sludges. Water Sci. Technol. 36, 9–18.

Slatter, P.T., 2001. Sludge pipeline design. Water Sci. Technol. 44, 115–120.

Tsutsumi, A., Yoshida, K., 1987. Effect of temperature on rheological properties of suspensions. J. Non-Newtonian Fluid Mech. 26, 175–183.

Wei, P., Tan, Q., Uijttewaal, W., van Lier, J.B., de Kreuk, M., 2018. Experimental and mathematical characterisation of the rheological instability of concentrated waste activated sludge subject to anaerobic digestion. Chem. Eng. J. 349, 318–326.